A facile synthesis of Co-doped g-C_3N_4 catalyst to activate peroxymonosulfate for organic pollutants degradation under visible light

Fangli Chi[1], Shengshu Ai[1], Fan Wang[1], Xiaona Ji[1], Dejun Bian[1]*

[1]Key Laboratory of Urban Sewage Treatment of Jilin Province, Changchun Institute of Technology, Changchun 130012, China

Abstract. Co-g-C_3N_4 catalyst was prepared by a simple calcination method using melamine and $Co(NO_3)_3 \cdot 6H_2O$ as precursors. X-ray diffraction (XRD), Fourier transform infrared spectra (FT-IR) were used to characterize the prepared samples. The results indicated the Co species are successfully coordinated with g-C_3N_4. Degradation experiments showed that Rhodamine B can be degraded effectively at a very low cobalt doping concentration (0.2 wt %). The enhanced catalytic activity may result from the synergistic effect of visible light photocatalysis and sulfate radical based Co-g-C_3N_4/PMS system.

1 INTRODUCTION

Advanced oxidation processes (AOPs) are considered as an attractive eco-environmental wastewater treatment technology. Among these processes, Fenton reaction (dissolved Fe(II) + H_2O_2) is mostly employed because it can produce hydroxyl radical (•OH) quickly which can degrade most organic compound into harmless chemicals such as CO_2 and H_2O. However, the production, transport and storage of H_2O_2 is expensive and this process is also restricted by its narrow working pH range (pH 2-3) and the production of large amounts of iron sludge[1]. Recently, sulfate radicals ($\bullet SO_4^-$)-based AOPs are becoming emerging alternatives to the common hydroxyl radicals (•OH)-based AOPs due to their strong redox potential (2.5–3.1V), wide working pH range (2-9) and better stability[2].

Peroxymonosulfate (PMS) is one of the widely-used reagent to produce $\bullet SO_4^-$. PMS can be activated by different methods, such as UV, heat, transition metals and metal-containing oxides, in which the method excited by transmission metal is most convenient. Among these transition metal ions Co^{2+} is very efficient to excite PMS to generate $SO_4^{\bullet-}$[3], however Co^{2+} is biological toxicity and recognized as a priority metal pollutant[4]. In order to solve this problem it was immobilized on various supports such as graphene[5], TiO_2[6],SiO_2[7], Bi_2O_3[8], and so on.

Graphitic carbon nitride (g-C_3N_4) is often applied as catalyst support[9]. More importantly, g-C_3N_4 can produce hydrogen or oxygen by water splitting and degrade organic pollutants under visible light irradiation due to its unique properties such as fast charge transfer, high thermal and chemical stability[10-13]. However, g-C_3N_4 suffers from some disadvantages, such as fast recombination of photogenerated electron-hole, low efficient visible-light utilization[14]. To improve the photocatalytic efficiency, many efforts have been done, for example, Sridharan synthesized C_3N_4/TiO_2 composite and found that the synergistic heterojunction formed between g-C_3N_4 nanosheets and TiO_2 can enhance electron transport and electron–hole pair separation efficiently[15]. Pan prepared $C_3N_4/BiPO_4$ photocatalyst and found that the composite possessed significantly enhanced photocatalytic activity due to the high separation and easy transfer of photogenerated electron–hole pairs at the heterojunction interfaces derived from the match of lattice and energy level between the C_3N_4 and $BiPO_4$[16].

In this study, Co-g-C_3N_4 catalyst with different Co concentration was prepared by a simple calcination method. The obtained samples were used as bifunctional catalyst for photocatalytic reaction and sulfate radicals ($\bullet SO_4^-$)-based AOPs. The synergistic effect resulted in significantly improved degradation rate of rhodamine B (RhB).

2 EXPERIMENT

2.1. Synthetic Procedures for Co-g-C_3N_4

The synthesis of Co/g-C_3N_4 material was carried out typically as follows: Melamine (2g) and different amount (0.2 wt %, 5.0 wt %) of $Co(NO_3)_3 \cdot 6H_2O$ were dissolved in 200 mL of deionized water and then stirring at 100 °C for 4 h until the water has been evaporated, a yellow-gray solid was obtained. Finally, the solid was transferred into a crucible, and the temperature of the furnace was elevated to 520 °C for 200 min and kept at 520 °C for 4 h under flowing Ar. The resultant yellow solid was kept in its original form and collected for further characterizations.

* Corresponding author: 394401207@qq.com

2.2. Sample Characterization.

X-ray diffraction (XRD) patterns were obtained on a Bruker D8-Advanecd X-ray diffractometer with Cu Kα radiation (λ= 1.5418 Å), at accelerating voltage and current of 40 kV and 30 mA, respectively. Scanning electron microscopy (SEM) was performed on a Zeiss Neon 40EsB FIBSEM. Fourier Transform IR Spectroscopy (FT-IR) was performed on a Nicoletis10 instrument (Thermo Nicolet Corporation).

2.3. Photocatalytic Degradation.

Photocatalytic activities of the samples were evaluated by the degradation of rhodamine B (RhB) under visible light irradiation of a 500 W Xe lamp. In a typical reaction run, the degradation experiments were carried out in 250 mL reactor containing. 0.1 g of photocatalyst was dispersed into 200 mL aqueous solution of RhB (5 mg L^{-1}) solution (a photo-Fenton-like reaction was initiated by adding 0.332 g peroxymonosulfate (using PMS, $KHSO_5$ from Aladdin) to the reactor). Before irradiation, the suspension was magnetically stirred in the dark for 5 min to achieve the adsorption–desorption equilibrium among the photocatalyst, RhB, and water. The RhB concentration after equilibration was determined by measuring the absorbance at 553 nm using a Perkin Elmer Lambda 750 UV/Vis/NIR spectrometer, and taken as the initial concentration (C_0). The reaction was kept at room temperature by cooling water to prevent any thermal catalytic effect. After the elapse of a period of time, 3 ml of the solution was taken, and the concentration (C) of RhB was measured.

3 RESULTS AND DISCUSSION

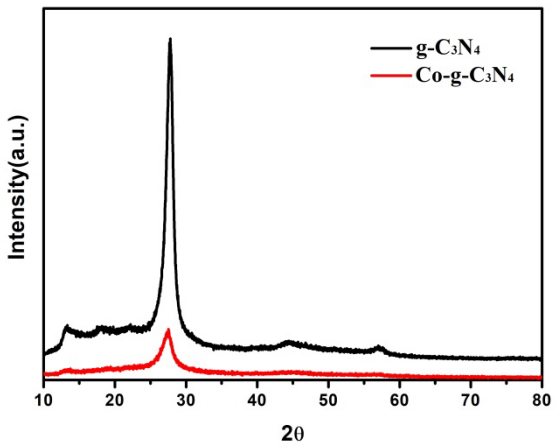

Fig.1. XRD patterns of g-C_3N_4 and Co-g-C_3N_4 samples

The XRD pattern of obtained g-C_3N_4 shows the strongest diffraction peak at 27.40 ° (d = 0.325 nm) (Fig. 1), which is a characteristic interlayer stacking peak of aromatic systems, indexed for graphitic materials as the (0 0 2) peak[10]. The peak at 13.08 °(d = 0.677 nm) is indexed as (1 0 0) peak that arises from the in-plane ordering of tri-s-triazine units[17]. After the incorporation of Co ions into g-C_3N_4 networks, the XRD pattern shows a significant intensity decrease, and together with the absence of the peak at ~13°, it suggests that cobalt ions are embedded into in-planes of carbon nitride sheets[18].

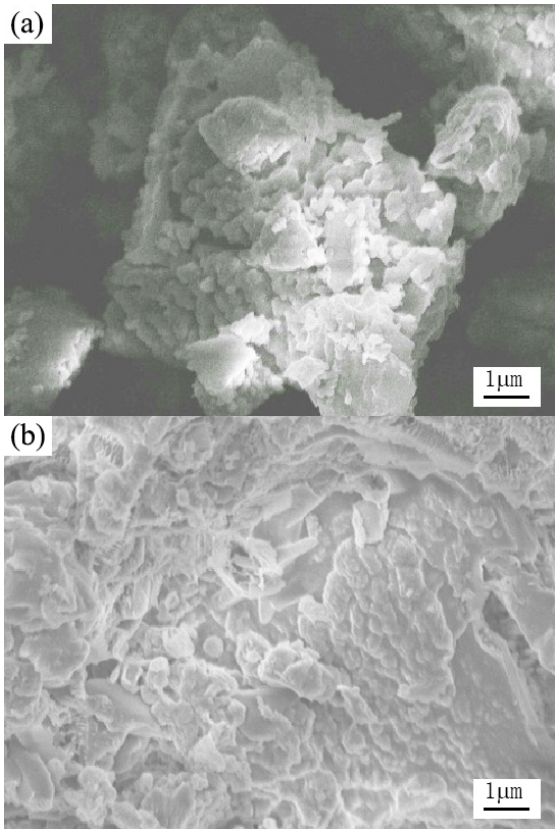

Fig.2. SEM images of (a) g-C_3N_4, (b) Co-g-C_3N_4

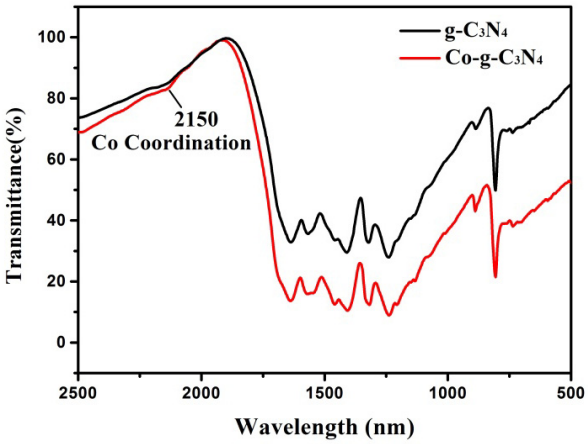

Fig.3. FT-IR spectra of g-C_3N_4 and Co-g-C_3N_4 samples.

The FT-IR spectra of Co-g-C_3N_4 and g-C_3N_4 are shown in Fig. 3. The strong absorption band in the range of 1200–1650 cm^{-1} is assigned to the typical skeletal stretching vibrations of the s-triazine or tri-striazine and the sharp peak centered at 808 cm^{-1} is a characteristic breathing mode of the triazine units [19]. These band were also found on the spectra of Co-g-C_3N_4, suggested that the original graphitic C−N network remains mostly unchanged after the inclusion of Co ions. Notably, an absorbance at ~2150 cm^{-1} is accompanied with the cobalt incorporation on the spectra of Co-g-C_3N_4, which

is ascribed to nitrile species. This verifies the incomplete polymerization aroused by Co coordination during the heat treatment[18].

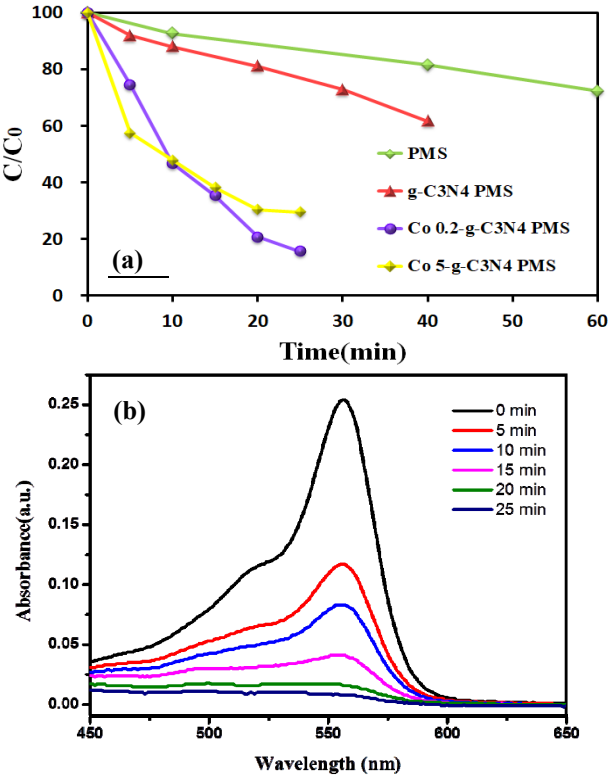

Fig.4. (a) photocatalytic degradation efficiencies of RhB as a function of irradiation time for the different samples. (b) Changes in UV-visible absorption spectra of RhB by Co0.2-g-C_3N_4.

Table 1. Degradation efficiency of RhB with different samples after 20 min of visible-light irradiation

Sample	g-C_3N_4	Co5-g-C_3N_4	Co0.2-g-C_3N_4
Degradation efficiency of RhB	18.9	69.5	79.4

RhB was selected as a model of organic pollutants to evaluate the degradation efficiency of Co-g-C_3N_4, the initial concentration of RhB is defined as C_0 while C is referred to the instantaneous concentration of RhB at different time. As shown in Fig.4, only 28% RhB was degraded after 60 min with PMS alone under visible-light irradiation. When g-C_3N_4 was added to the system, 38% RhB was degraded after 40 min of visible-light irradiation. When 0.2 wt % Co doped g-C_3N_4 was used as the catalyst, the degradation rate of RhB has been improved to 85% after only 25 min of visible-light irradiation. As shown in Fig. 4 and table 1, the C/C_0 values of g-C_3N_4, Co5-g-C_3N_4 and Co0.2-g-C_3N_4 are 18.9%, 69.5% and 79.4% at the 20th minute of the reaction time. This dramatic improvement result from the synergistic effect between g-C_3N_4 photocatalytic reaction and $\bullet SO_4^-$ produced from PMS which can be activated by Co ions more effectively. However, 5.0 wt % Co-g-C_3N_4 exhibits lower photocatalytic activity compared with 0.2 wt % Co-g-C_3N_4, which may be explained by the agglomeration and lower dispersibility of Co species[20]. Therefore, an appropriate doping level of Co in the g-C_3N_4 is critical.

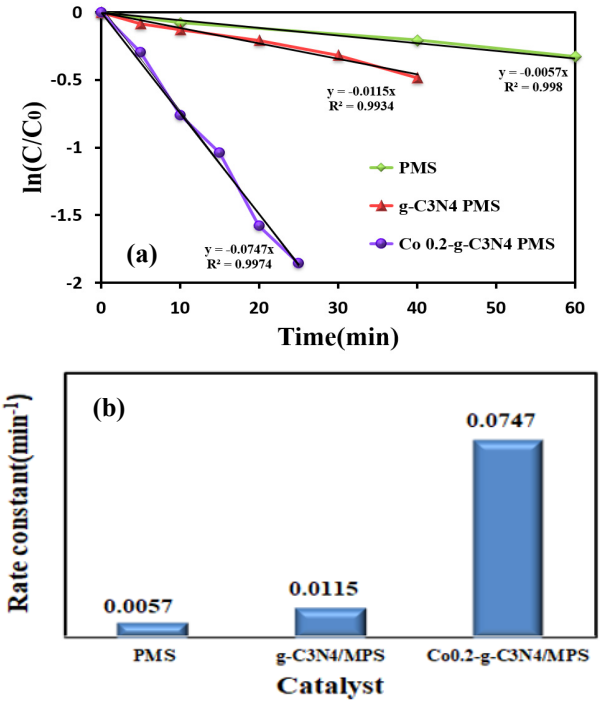

Fig.5. (a) Kinetic curves and (b) reaction rate constant of the PMS, g-C_3N_4/PMS, Co0.2-g-C_3N_4/PMS for the degradation of RhB.

The kinetic study of degradation of RhB was also investigated and fitted by first order reaction kinetic model, as shown in Fig. 5(a) and (b). The rate constant of the RhB degradation with PMS, g-C_3N_4/PMS, Co0.2-g-C_3N_4/PMS is estimated to be 0.0057, 0.0115, 0.0747, min^{-1}, respectively. The corresponding R^2 (correlation coefficient) values are 0.998, 0.993 and 0.997, respectively, which are close to 0.99, proving that the reaction is in line with the proposed rate law for RhB degradation. The k value for the Co0.2-g-C_3N_4/PMS sample is about 6.50 times that of the g-C_3N_4. The results showed that Co/g-C_3N_4/PMS were more effective in the degradation of RhB.

4 CONCLUSIONS

Co-g-C_3N_4 catalyst has been successfully synthesized by a simple calcination method. XRD and FT-IR indicated the Co species are successfully coordinated with g-C_3N_4. Compared with g-C_3N_4, Co-g-C_3N_4 demonstrates higher catalytic activity to activate PMS, when 0.2 wt % Co doped g-C_3N_4 used as catalyst, the degradation rate of RhB improved to 85% after only 25 min of visible-light irradiation. The enhanced catalytic activity may result from the synergistic effect of visible light photocatalysis and $\bullet SO_4^-$ based Co-g-C_3N_4/PMS system. However, 5.0 wt % Co-g-C_3N_4 exhibits lower degradation rate. Therefore, an appropriate doping level of Co in the g-C_3N_4 is critical.

Acknowledgements

This work was supported by the National Natural Science Foundation of China (51878067), Science and Technology Project of Jilin Provincial Department of Education (JJKH20200632KJ), Jilin Provincial Science & Technology Department (202002030JC).

References

1. Wang, N.; Zheng, T.; Zhang, G.; Wang, P. *J. Environ. Chem. Eng.* **4**,762, (2016).
2. Xia, D.; Yin, R.; Sun, J.; An, T.; Li, G.; Wang, W.; Zhao, H.; Wong, P. K. *J. Hazard. Mater.* **340**,435, (2017).
3. Cai, C.; Zhang, H.; Zhong, X.; Hou, L. W. *J. Hazard. Mater.* **283**,70, (2015).
4. Shi, P. H.; Su, R. J.; Zhu, S. B.; Zhu, M. C.; Li, D. X.; Xu, S. H. *J. Hazard. Mater.* **229**,331, (2012).
5. Yao, Y.; Yang, Z.; Sun, H.; Wang, S. *Ind. Eng. Chem. Res.* **51**,14958, (2012).
6. Zhu, Y.; Chen, S.; Quan, X.; Zhang, Y. *Rsc Adv.* **3**,520, (2013).
7. Hu, L.; Yang, X.; Dang, S. *Appl. Catal. B-Environ.* **102**,19, (2011).
8. Ding, Y.; Zhu, L.; Huang, A.; Zhao, X.; Zhang, X.; Tang, H. *Catal. Sci. Technol.* **2**,1977, (2012).
9. Su, X.; Vinu, A.; Aldeyab, S. S.; Zhong, L. *Catal. Lett.* **145**,1388, (2015).
10. Yan, S. C.; Li, Z. S.; Zou, Z. G. *Langmuir* **25**,10397, (2009).
11. Yan, S. C.; Li, Z. S.; Zou, Z. G. *Langmuir* **26**,3894, (2010).
12. Xiang, Q. J.; Yu, J. G.; Jaroniec, M. *J. Phys. Chem. C* **115**,7355, (2011).
13. Wang, X.; Maeda, K.; Thomas, A.; Takanabe, K.; Xin, G.; Carlsson, J. M.; Domen, K.; Antonietti, M. *Nat. Mater.* **8**,76, (2009).
14. Liu, G.; Niu, P.; Sun, C.; Smith, S. C.; Chen, Z.; Lu, G. Q.; Cheng, H.-M. *J Am. Chem. Soc.* **132**,11642, (2010).
15. Sridharan, K.; Jang, E.; Park, T. J. *Appl. Catal. B-Environ.* **142**,718, (2013).
16. Pan, C. S.; Xu, J.; Wang, Y. J.; Li, D.; Zhu, Y. F. *Adv. Funct. Mater.* **22**,1518, (2012).
17. Min, S. X.; Lu, G. X. *J. Phys. Chem. C* **116**,19644, (2012).
18. Liu, Q.; Zhang, J. *Langmuir* **29**,3821, (2013).
19. Thomas, A.; Fischer, A.; Goettmann, F.; Antonietti, M.; Muller, J.-O.; Schlogl, R.; Carlsson, J. M. *J. Mater. Chem.* **18**,4893, (2008).
20. Shao, H.; Zhao, X.; Wang, Y.; Mao, R.; Wang, Y.; Qiao, M.; Zhao, S.; Zhu, Y. *Appl. Catal. B-Environ.* **218**,810, (2017).